Journal of Vertebrate Paleontology
Publication details, including instructions for authors and subscription information:
http://www.tandfonline.com/loi/ujvp20

The first enantiornithine bird from the Upper Cretaceous of China

Min Wang [a b], Zhonghe Zhou [a] & Guanghui Xu [a]

[a] Key Laboratory of Vertebrate Evolution and Human Origins, Institute of Vertebrate Paleontology and Paleoanthropology, Chinese Academy of Sciences, Beijing, 100044, China

[b] University of Chinese Academy of Sciences, Beijing, 100044, China

Published online: 07 Jan 2014.

To cite this article: Min Wang, Zhonghe Zhou & Guanghui Xu (2014) The first enantiornithine bird from the Upper Cretaceous of China, Journal of Vertebrate Paleontology, 34:1, 135-145

To link to this article: http://dx.doi.org/10.1080/02724634.2013.794814

Journal of Vertebrate Paleontology 34(1):135–145, January 2014

ARTICLE

THE FIRST ENANTIORNITHINE BIRD FROM THE UPPER CRETACEOUS OF CHINA

MIN WANG,*[,1,2] ZHONGHE ZHOU,[1] and GUANGHUI XU[1]
[1]Key Laboratory of Vertebrate Evolution and Human Origins, Institute of Vertebrate Paleontology and Paleoanthropology, Chinese Academy of Sciences, Beijing 100044, China, wangmin_nju@163.com; zhouzhonghe@ivpp.ac.cn; xuguanghui@ivpp.ac.cn;
[2]University of Chinese Academy of Sciences, Beijing 100044, China

ABSTRACT—A new Late Cretaceous avian taxon, *Parvavis chuxiongensis*, gen. et sp. nov., is reported here based on an incomplete skeleton from Upper Cretaceous lake deposits in Yunnan Province, southern China. A phylogenetic analysis of 32 taxa and 242 morphological characters resulted in three most parsimonious trees, the strict consensus tree of which places *Parvavis chuxiongensis* within Enantiornithes. Histological study shows that the bones of *Parvavis* were composed of parallel-fibered bone tissue without lines of arrested growth, and indicated that growth rate had slowed but had not stopped at any stage prior to death. The bones also lack the rough surface texture seen in juvenile birds. Therefore, the new bird was probably close to adult body size at the time of death. However, the specimen is surprisingly small, highlighting the wide range of body sizes in Upper Cretaceous enantiornithines. The new specimen also represents both the first known bird from the Upper Cretaceous of China and the first Mesozoic bird from the south of China, and thus extends the temporal and geographic range of Mesozoic birds in China.

SUPPLEMENTAL DATA—Supplemental materials are available for this article for free at www.tandfonline.com/UJVP

INTRODUCTION

A large number of enantiornithine birds have been discovered and named in the last three decades, since the subclass Enantiornithes was established by Walker (1981), making the known diversity of Enantiornithes greater than that of any other avian clade during the Mesozoic. As one of the world's most important terrestrial fossil lagerstätten, the Jehol Group (131–120 Ma) has yielded numerous and exquisitely preserved Lower Cretaceous birds (Zhou, 2006; Zhou and Zhang, 2006a) that have greatly enriched our understanding of the early avian radiation (M. Zhang et al., 2001; Zhou et al., 2003; Zhou and Zhang, 2006a). The Jehol bird fauna includes over a dozen genera that can be referred to Enantiornithes, including *Cathayornis* (Zhou et al., 1992), *Protopteryx* (F. Zhang and Zhou, 2000), *Longipteryx* (F. Zhang et al., 2001), *Pengornis* (Zhou et al., 2008), and *Shanweiniao* (O'Connor et al., 2009). The Jehol Biota includes the majority of the known Enantiornithes from China, with only a few exceptions. However, *Otogornis genghisi* Hou, 1994, and *Cathayornis chaobuensis* Li, Li, Zhang, Zhou, Bai, Zhang, and Ba, 2008, are from the Lower Cretaceous of Inner Mongolia and *Qiliania* and several unnamed enantiornithine specimens are known from the Lower Cretaceous Xiagou Formation in Gansu Province (You et al., 2005, 2010; Harris et al., 2006; Lamanna et al., 2006; Ji et al., 2011). All of the above records are restricted to northern China. Here we report the first Mesozoic bird from southern China.

The skeleton was collected by one of us (G.X.) in 2010 from the Jiangdihe Formation at Luojumei Village, Chuxiong City, in Yunnan Province, southern China (Fig. 1). Mesozoic strata are widely exposed in Yunnan Province, with Jurassic and Cretaceous strata cropping out mainly in the center of the province. The fossil-bearing Jiangdihe Formation is composed of purple sandy mudstone with interbedded shale, with siltstone and sandstone appearing in the upper portion. The Jiangdihe Formation is conformable with both the underlying Matoushan Formation and the overlying Zhaojiadian Formation. The litho- and biostratigraphic correlation performed by the regional geological survey suggests that the Jiangdihe Formation was deposited during the Late Cretaceous (Y. Zhang, 1996), a conclusion corroborated by evidence from fossil invertebrates (conchostracans: e.g., *Aglestheria*, *Halysestheria*, *Nemestheria*; ostracods: e.g., *Cypridea*, *Limnocythere*) and palynomorphs that indicate the formation is Turonian–Santonian in age (Chen, 2000).

Institutional Abbreviations—**BMNH**, Beijing Museum of Natural History, Beijing, China; **CAGS-IG**, Institute of Geology, Chinese Academy of Geological Sciences, Beijing; **DNHM**, Dalian Natural History Museum, Dalian, China; **GMV**, National Geological Museum of China, Beijing; **LH**, Las Hoyas Collection, Museo de Cuenca, Cuenca, Spain; **NIGP CAS**, Nanjing Institute of Geology and Paleontology, Chinese Academy of Sciences, Nanjing, China; **STM**, Tianyu Natural History Museum, Shandong, China; **IVPP**, Institute of Vertebrate Paleontology and Paleoanthropology, Beijing, China.

MATERIALS AND METHODS

Anatomical terminology follows Baumel and Witmer (1993), using English equivalents of Latin terms. Terminology for structures not named therein follows Howard (1929). Measurements given in this paper are maximum lengths, each taken along the longitudinal axis of the bone; for an ungual phalanx, the measurement represents the linear distance between the proximal end of the element and the tip of the horny sheath.

Three histological samples were taken from the midshafts of the right humerus (two) and right ulna (one) using a microsaw. The samples were then embedded in EXAKT Technovit 7200 one-component resin, allowed to dry for 21 hours, and cut and polished until the desired optical contrast was obtained. The finished transverse sections were examined and photographed

*Corresponding author.
Color versions of one or more of the figures in the article can be found online at www.tandfonline.com/ujvp.

FIGURE 1. Map of China showing fossil locality. The holotype of *Parvavis chuxiongensis*, gen. et sp. nov (IVPP V18586) was found in Luojumei Village, 14 km east of Chuxiong City in Yunnan Province.

under both the normal and polarized light using a Leica DM-RX polarizing microscope.

A phylogenetic analysis was performed using the data matrix of O'Connor et al. (2009), with character states for the new specimen and two basal ornithuromorphs (*Archaeorhynchus* and *Songlingornis*) added in. The expanded data matrix was composed of 32 taxa and 242 characters. Dromaeosauridae was used as the outgroup, and Neornithes was represented by *Anas platyrhynchos* and *Gallus gallus*. Thirty-one characters were considered ordered and 23 uninformative characters were removed from the analysis (leaving 219 characters), following O'Connor et al. (2009). Twenty-nine characters were scored for the new species, and the character states scored for *Archaeorhynchus* and *Songlingornis* were based on You et al. (2010) (Appendix 1 and Supplementary Data).

We explored the possibility of using the enlarged matrix of O'Connor and Zhou (2013) with *Parvavis* added in, but recovered little resolution within Ornithothoraces (even the monophyly of both Enantiornithes and Ornithuromorpha was broken down). Although the matrix used in our analysis, based on that of O'Connor et al. (2009), did not contain all known enantiornithines, it was larger than those used in many previous studies (Chiappe et al., 2007a; Zhou et al., 2008). Some enantiornithine taxa were excluded from our analysis, which were not included in the O'Connor et al. (2009) matrix, because they are either represented by poorly preserved specimens (e.g., *Otogornis*, *Eocathayornis*, *Boluochia*), are controversial (e.g., *Cathayornis* is regarded as a synonym of *Sinornis* by Sereno et al. [2002]), or could not be studied firsthand (e.g., *Shenqiornis*, *Bohaiornis*). Because including taxa that are too fragmentary or otherwise problematic can result in a profusion of equally parsimonious trees and a highly polytomous strict consensus tree, so obscuring true relationships (Wilkinson, 2003), we prefer the reduced data set here used.

The phylogenetic analysis was performed with TNT version 1.1 (Goloboff et al., 2008). We used unconstrained traditional searches, with 1000 replicates of random stepwise addition (branch swapping: tree-bisection-reconnection) and 10 trees were held at each step. All characters were given equal weight, and branches with minimum branch lengths of zero were collapsed to create polytomies. Bootstrap and Bremer values were calculated as indices of support. Bootstrapping was conducted with 1000 replicates, with the same settings that were used for the primary search. Absolute Bremer support (Bremer, 1994) for each clade was calculated using an unweighted analysis, and the resulting values indicate how many extra steps would be required to reject the monophyly of each clade. The strategy of Giannini et al. (2004) was applied here. We explored suboptimal trees by performing an initial search for trees one step longer than the optimals, then a second search for trees two steps longer, and so on, until the eighth search for trees eight steps longer. During each search, 2000 trees were retained. The total number of suboptimal trees (about 16,000) was large enough to effectively prevent overestimation of Bremer values.

SYSTEMATIC PALEONTOLOGY

AVES Linnaeus, 1758
ENANTIORNITHES Walker, 1981
PARVAVIS, gen. nov.

Type Species—*Parvavis chuxiongensis*, gen. et sp. nov.

Etymology—The genus name is from 'parv' Latin prefix for 'small,' and 'avis,' Latin for 'bird.'

Diagnosis—As for the type and only species.

Distribution—As for the type and only species.

PARVAVIS CHUXIONGENSIS, gen. et sp. nov.
(Figs. 2, 3)

Holotype—An articulated partial skeleton preserved in a slab (IVPP V18586/1) (Fig. 2) and counter slab (IVPP V18586/2) (Fig. 3) with feather impressions covering the body cranial to the pygostyle.

Locality and Horizon—Luojumei Village, Chuxiong City, Yunnan Province, China. Jiangdihe Formation, Upper Cretaceous (Turonian–Santonian) (Chen, 2000).

Etymology—The species name refers to the city of Chuxiong, where the fossil was collected.

Differential Diagnosis—An enantiornithine because it has autapomorphies of this clade, as follows: proximal profile of humerus concave, cranial facies immediately distal to head concave, deltopectoral crest narrower than shaft width, and ventral side of distal humerus extending more distally than dorsal side. A small species, with humerus less than half as long as that of *Longipteryx*, distinguished from other known enantiornithine birds by the following combination of characters: metatarsals II and IV terminate proximal to the entire trochlea of metatarsal III; the trochlea of metatarsal II broader than those of other metatarsals (widely distributed in enantiornithines, e.g., *Eoenantiornis*, *Vescornis*); and ungual of digit IV reduced (among other enantiornithines, found only in *Vescornis* and *Qiliania*).

ANATOMICAL DESCRIPTION AND COMPARISONS

Skull

Only the occipital region of the skull is preserved, and is exposed in occipital view and is severely damaged (Fig. 2). Only a few enantiornithines, including *Vescornis hebeiensis*, *Neuquenornis volans*, and *Shenqiornis mengi* (Chiappe and Calvo, 1994; F. Zhang et al., 2004; O'Connor and Chiappe, 2011), are currently represented by specimens that reveal the structure of the occiput. The foramen magnum is pentagonal as in *Shenqiornis*, but differs

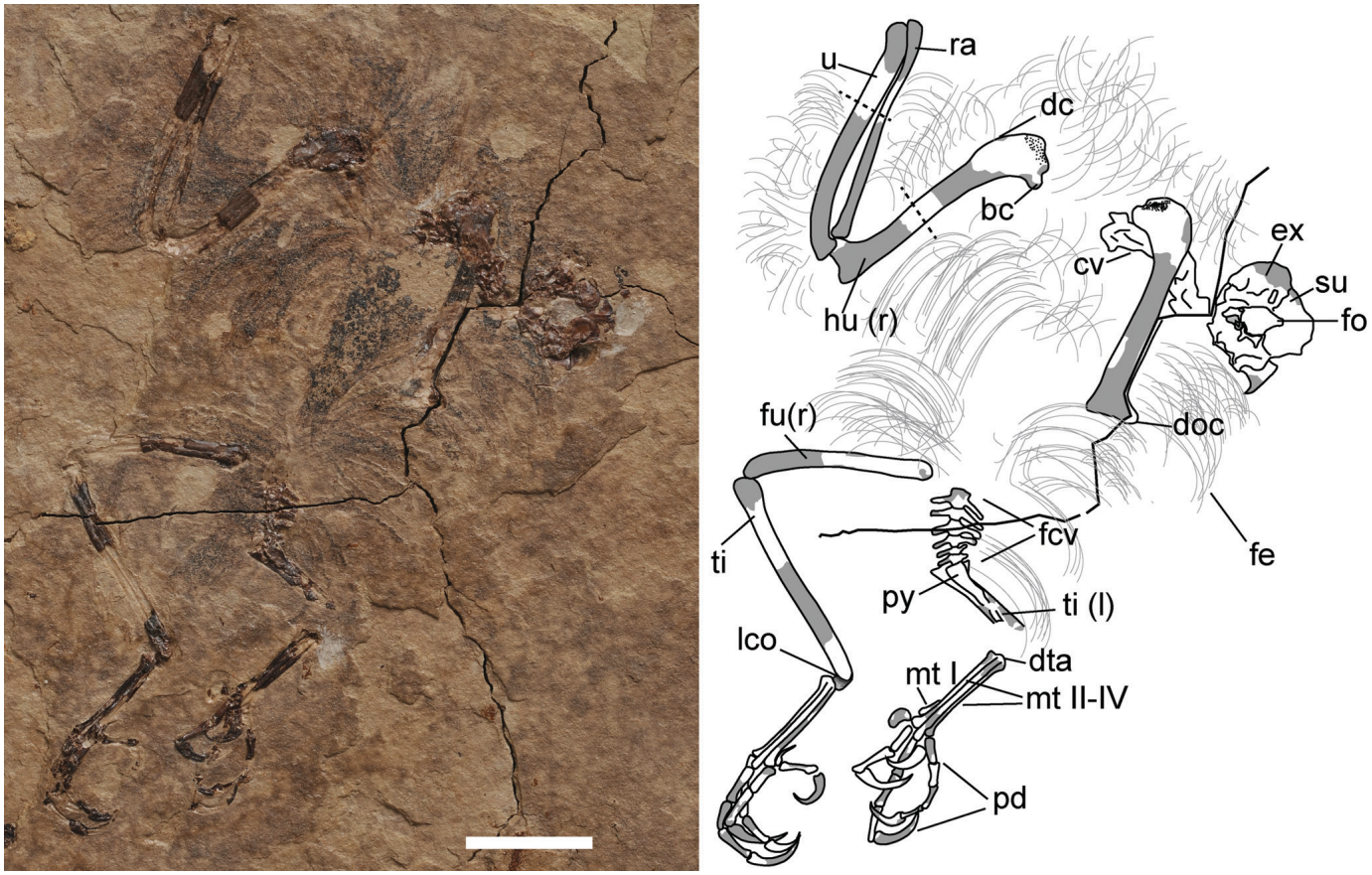

FIGURE 2. Photograph and line drawing, where shaded parts indicate missing bone, of IVPP V18586/1 (part), holotype of *Parvavis chuxiongensis*, gen. et sp. nov. **Abbreviations**: **bc**, bicipital crest; **cv**, cervical vertebrae; **dc**, deltopectoral crest; **doc**, dorsal condyle; **dta**, distal tarsals; **ex**, exoccipital; **fcv**, free caudal vertebrae; **fe**, feather impression; **fo**, foramen magnum; **fu**, femur; **hu**, humerus; **l**, left side; **lco**, lateral condyle; **mt I–IV**, metatarsals I–IV; **pd**, pedal digit; **py**, pygostyle; **r**, right side; **ra**, radius; **su**, supraoccipital; **ti**, tibiotarsus; **u**, ulna. Dashed lines indicate locations histological sections. Scale bar equals 10 mm.

from those of both *Vescornis* and *Shenqiornis* (O'Connor and Chiappe, 2011) in being taller dorsoventrally than wide mediolaterally. Proportional to the size of the occipital region, the foramen magnum is comparable in size to that of *Shenqiornis* and much larger than in *Vescornis*. The dorsal margin of the foramen magnum is formed by the supraoccipital, whereas the lateral margins are formed by fragmentary bones that probably represent the exoccipitals. In *Shenqiornis*, the exoccipitals form the lateral margins and the entire ventral margin of the foramen magnum (O'Connor and Chiappe, 2011). The bones ventral to the foramen magnum in *Parvavis* are fragmentary and may represent exoccipitals or the basioccipital. No clear cerebellar prominence (exists in *Neuquenornis*) is visible in the supraoccipital, but the absence of this structure in *Parvavis* may be a result of poor preservation. The occipital condyle is worn away.

Axial Skeleton

Several articulated vertebrae situated near the skull are interpreted as cervicals (Fig. 2). Poor preservation and the fact that the left humerus overlies these vertebrae prevent recognition of any important anatomical features.

Six articulated vertebrae, as counted by their transverse processes, are preserved in articulation with the pygostyle (Fig. 2). The number of vertebrae situated cranial to the pygostyle in *Parvavis* falls within the range of free caudal counts known in other enantiornithines. There are six free caudal vertebrae in *Sinornis* and *Rapaxavis* (Sereno et al., 2002; O'Connor et al., 2011), six or seven in *Protopteryx* (F. Zhang and Zhou, 2000), and eight in *Iberomesornis* (Sanz et al., 2002). Of the juvenile enantiornithine specimens described by Chiappe et al. (2007b), there are at least seven free caudals in GMV-2158, and seven in GMV-2156/NIGP130723 (Chiappe et al., 2007b). For these reasons, and because there is no indication of fusion between these vertebrae, we interpret them as free caudals. However, it is possible that additional free caudal vertebrae were present in the complete skeleton. The transverse processes are slightly caudally directed, and become craniocaudally narrow in the more caudally located vertebrae. The lengths of the transverse processes of the cranial-most four vertebrae in the series equal or surpass the width of each corresponding centrum. The pygostyle is damaged, leaving few details discernible.

Thoracic Limb

The humeri are partially preserved on both the part and counterpart slabs. The proximal ends of both humeri are well preserved on IVPP V18586/1 in cranial view (Fig. 2), leaving impression on the counter slab. A cast was prepared from the counterpart in order to reveal more details of the cranial surface of the proximal ends of both humeri (Fig. 4B) and forms the basis of our description of the proximal end. The proximal margin shows

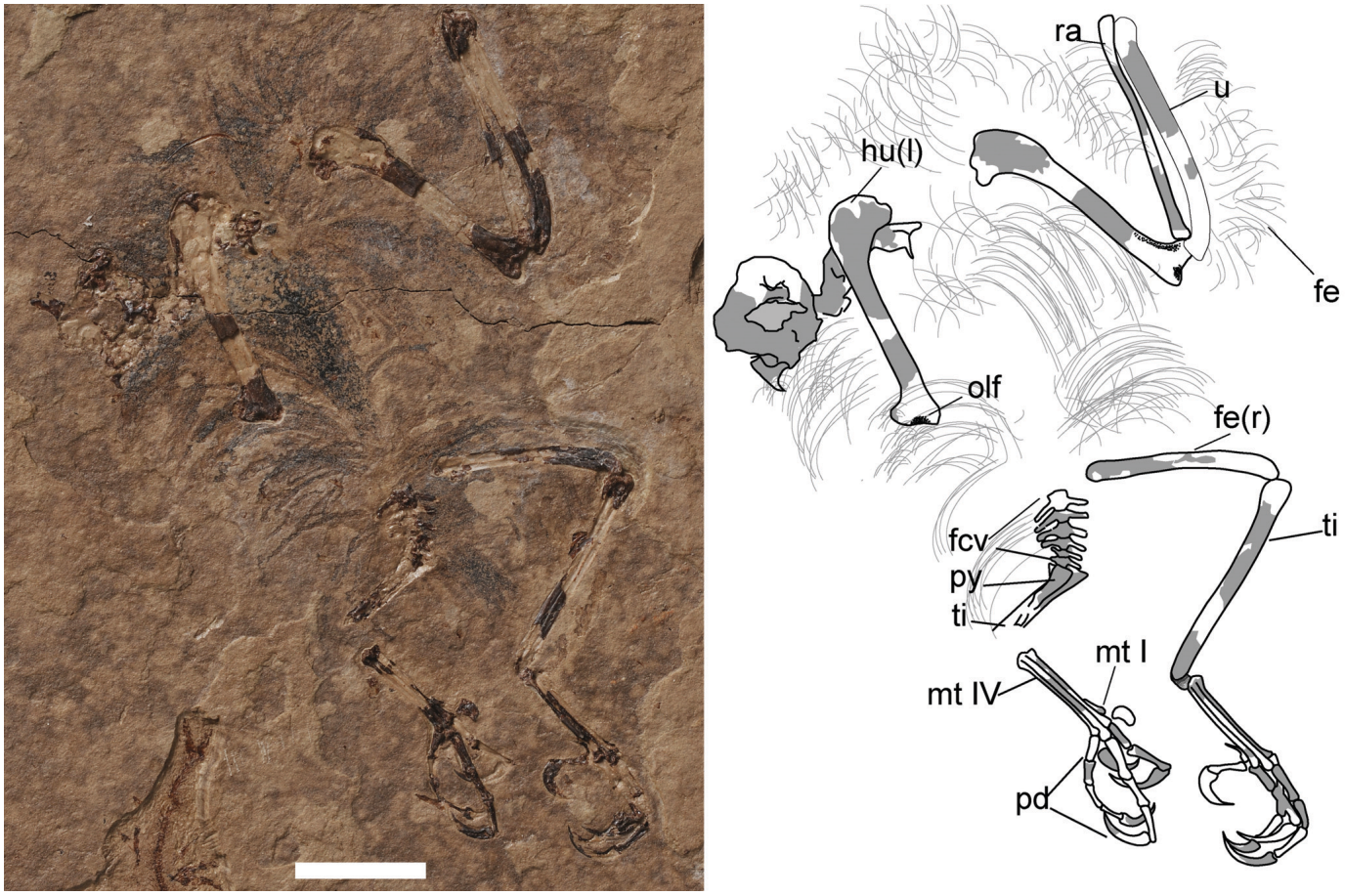

FIGURE 3. Photograph and line drawing, where shaded parts indicate missing bone, of IVPP V18586/2 (counterpart), holotype of *Parvavis chuxiongensis*, gen. et sp. nov. **Abbreviations**: **fcv**, free caudal vertebrae; **fe**, feather impression; **fu**, femur; **hu**, humerus; **l**, left side; **mt I–IV**, metatarsals I–IV; **olf**, olecranon fossa; **pd**, pedal digit; **py**, pygostyle; **r**, right side; **ra**, radius; **ti**, tibiotarsus; **u**, ulna. Scale bar equals 10 mm.

the typical enantiornithine condition in having a slightly concave central part bound by proximally elevated adjacent dorsal and ventral regions of the head (Chiappe and Walker, 2002). The only enantiornithine that does not display this pattern is *Pengornis houi*, which has a globose humeral head similar to that seen in ornithurines (Zhou et al., 2008). A depression on the cranial facies flanked dorsally and ventrally by prominences lies slightly distal to the humeral head, rendering it concave as in other enantiornithine birds (Chiappe and Walker, 2002). The bicipital crest is well developed, projects cranioventrally, and is separated from the humeral head by a shallow capital incision. The deltopectoral crest is weakly developed as in *Elsornis* (Chiappe et al., 2007a) and the three juvenile specimens described by Chiappe et al. (2007b): this structure projects from the shaft less than half shaft width and its length is less than one-third of that of the humeral shaft in *Parvavis* and the juvenile specimens, and is even weaker in *Elsornis*. In contrast, the deltopectoral crest is well developed (longer and more projecting) in other enantiornithines, including *Longipteryx*, *Vescornis*, *Pengornis*, and *Eocathayornis* (F. Zhang et al., 2001, 2004; Zhou, 2002; Zhou et al., 2008) (Fig. 4). The deltopectoral crest tapers distally and recedes gently into the shaft as in *Rapaxavis* and *Eoenantiornis* (Zhou et al., 2005; Morschhauser et al., 2009), in contrast with the abrupt ending seen in *Enantiornis*, the El Brete species, *Shenqiornis*, *Protopteryx*, and an unnamed species from the Xiagou Formation of China (CAGS-IG-02-0901) (Walker, 1981; F. Zhang and Zhou, 2000; Chiappe and Walker, 2002; You et al., 2005; Walker et al., 2007; Wang et al., 2010) (Fig. 4). The distal humeri are well exposed in caudal view on IVPP V18586/2 (Figs. 3, 4A). The dorsal condyle projects dorsally and the ventral epicondyle extends farther distally than the dorsal one, making the distal surface of the humerus proximodorsally angled as in *Vescornis*, *Longipteryx*, and the El Brete species. The right humerus bears a groove lateral to the shallow olecranon fossa and near to the dorsal margin. It apparently extended proximally beyond the point at which the distal fragment is broken away from the rest of the bone. We interpret this feature as a scapulotricipital groove, based on comparisons with modern birds that take into account its position and morphology (following Zhou, 1995; contra Chiappe and Walker, 2002).

The right ulna and radius remain in articulation with the humerus (Fig. 4A). The ulna slightly surpasses the humerus and radius in length. The distal part of the ulnar shaft is straight but the proximal part is bowed caudally, creating a wider interosseous space proximally between the ulna and radius. The ulna is exposed in dorsal aspect, with few identifiable features visible. Quill knobs for the attachment of the secondary feathers are not visible, even under magnification. The rod-like radius is approximately half of the width of the ulna as in most Enantiornithes. A relatively more robust radius, measuring more than 70% of the width of the ulna, is present in *Eocathayornis*, *Pengornis*, and *Rapaxavis* (Zhou, 2002; Zhou et al., 2008; O'Connor et al., 2009). Because the radius is fragmentary, and essentially

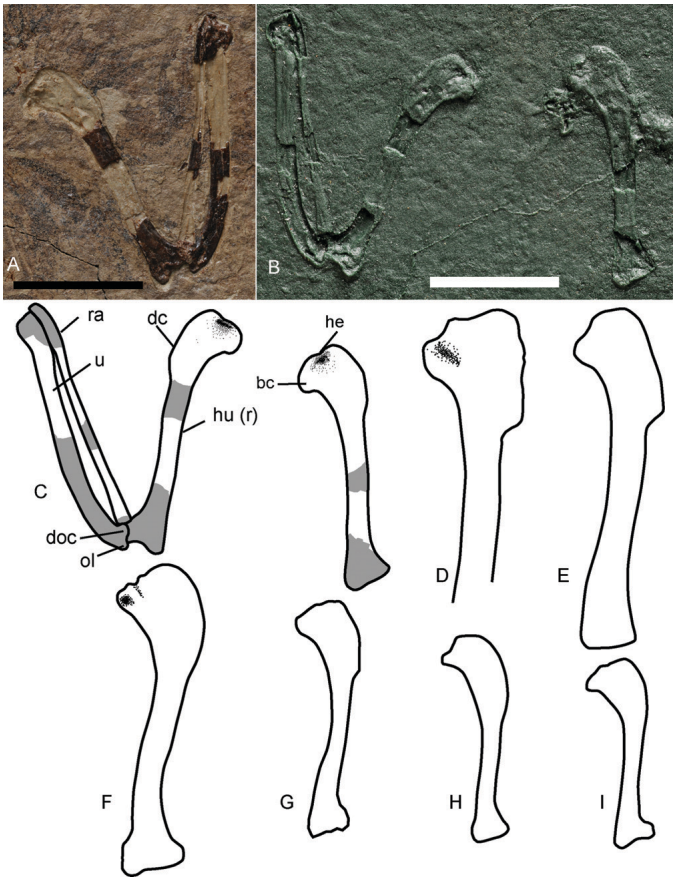

FIGURE 4. Comparisons among the humeri of some enantiornithines. **A** and **B**, photographs of **A**, right humerus IVPP V18586/2 in caudal view; **B**, cast of the cranial surface of the proximal humerus of IVPP V18586/2. **C**–**H**, line drawings in cranial view of the humeri of the following specimens and taxa: **C**, IVPP V18586, holotype of *Parvavis chuxiongensis*, gen. et sp. nov.; **D**, *Enantiornis leadi* (modified from Walker et al., 2007); **E**, DNHM D2950, holotype of *Shenqiornis mengi* (modified from Wang et al., 2010); **F**, IVPP V9607, holotype of *Otogornis genghisi*; **G**, IVPP V9769, holotype of *Cathyornis yandica*; **H**, IVPP V12325, holotype of *Longipteryx chaoyangensis* (modified from F. Zhang et al., 2001); **I**, IVPP V11537, holotype of *Eoenantiornis buhleri*. **Abbreviations**: **bc**, bicipital crest; **dc**, deltopectoral crest; **doc**, dorsal condyle; **he**, humeral head; **hu**, humerus; **ol**, olecranon; **r**, right side; **ra**, radius; **u**, ulna. All scale bars equal 10 mm. **C**–**I** are not to scale.

exposed in two dimensions, it is difficult to determine whether the interosseous surface bears the longitudinal groove that is synapomorphic for Enantiornithes (Chiappe and Walker, 2002).

Pelvic Limb

The intermembral ratio (humerus + ulna/femur + tibiotarsus) is 1.15. The proximal end of the right femur is partially preserved and exposed in medial view. Thus, the characteristic enantiornithine trochanter, located posterolaterally near the proximal end of the femur (Chiappe and Walker, 2002), cannot be observed. The femur is long, measuring more than 80% of the length of the tibiotarsus, and its shaft is bowed cranially as in most enantiornithines. The femur is nearly straight in the juvenile specimens described by Chiappe et al. (2007b), which suggests that the femur becomes bowed during ontogeny (Ji et al., 2011).

The tibiotarsi are poorly preserved. Only the proximal part of the left tibiotarsus is preserved, and this fragment is overlain by the crushed pygostyle (Fig. 2). The right tibiotarsus is preserved in lateral view, revealing the articular facet for the femur. The articular facet seems to be flat, but is angled to face slightly laterally. A cnemial crest cannot be seen. Erosion at the distal end makes it impossible to determine to what degree the proximal tarsals are fused with the tibia. The lateral condyle protrudes well beyond the cranial surface of the shaft.

The distal tarsals are fused into a tarsal cap, which articulates tightly against the proximal ends of the three major metatarsals. However, a suture line is visible between the tarsal cap and metatarsals (Fig. 5), so the tarsometatarsus is not fused proximally. Free distal tarsals are still relatively rare among Mesozoic birds, having only recently been definitively reported for five taxa: *Archaeopteryx* (Wellnhofer, 1992), *Rahonavis* (Forster et al., 1998), the juvenile enantiornithine GMV-2158 (Chiappe et al., 2007b), *Shenqiornis* (Wang et al., 2010), and *Rapaxavis* (O'Connor et al., 2011). Their existence in *Iberomesornis* is still controversial (Sanz and Bonaparte, 1992; Sereno, 2000). The tarsal cap covers metatarsals III and IV. Metatarsals II through IV are exposed in dorsal view in IVPP V18586/1, and leave the proximal and distal ends of the left metatarsals in plantar view in V18586/2. Although tightly abutting each other, metatarsals II–IV are not fused along their length. Metatarsal fusion is a function of ontogeny, and metatarsals II–IV are usually only fused proximally in enantiornithines (Chiappe and Walker, 2002). The presence of suture lines between the plantar surfaces of the proximal ends of metatarsals II–IV indicates that these elements are not fused proximally. Among the three major metatarsals, metatarsal III is the longest, at about half the length of the tibiotarsus. Metatarsals II and IV are subequal in length, and terminate entirely proximal to the trochlear portion of metatarsal III. The shaft of metatarsal II is as wide as that of metatarsal III. The trochlea of metatarsal II is slightly wider than that of metatarsal III, and considerably wider than that of metatarsal IV. The dorsal surface of metatarsal III is convex. The shaft of metatarsal IV is transversely narrower than those of the other two major metatarsals, a common feature in enantiornithines. The right metatarsal I is exposed in mediodorsal view in IVPP V18586/1, and its curvature suggests a 'J'-shaped morphology.

The feet are preserved in natural articulation, and are nearly complete (Fig. 5). The pedal phalangeal formula is 2-3-4-5-x. The hallux is slender and reversed. The penultimate phalanx of digit II is robust, and is longer than the preceding phalanx. Digit III is the longest of the digits, followed by digit II, and both are longer than metatarsal III. The proximal phalanx of digit III and the penultimate phalanx of digit II are of equal length and represent the longest non-ungual phalanges. The non-ungual phalanges of digit IV are slender and relatively short compared with those of the other digits. The proximal two phalanges are about equal in length, and are slightly shorter than the distal two phalanges. The unguals are much longer than the preceding phalanges in their respective digits when the horny sheaths are taken into account, but lack strong curvature and well-developed flexor tubercles. Longitudinal crests are visible ventral to the neurovascular sulcus of the unguals, and equivalent structures have been reported in other enantiornithines, including *Rapaxavis*, *Shanweiniao*, and *Qiliania* (O'Connor et al., 2009, 2011; Ji et al., 2011). The ungual of digit IV is reduced compared with those of the other three digits, a feature also known in *Vescornis* and *Qiliania* within enantiornithines (F. Zhang et al., 2004; Ji et al., 2011).

Integument

Feathers are preserved as carbonized traces, and cover most of the body cranial to the pygostyle (Figs. 2, 3). Although the detailed structure of the feathers is not clear, they are curved and comparable to the major metatarsals in length.

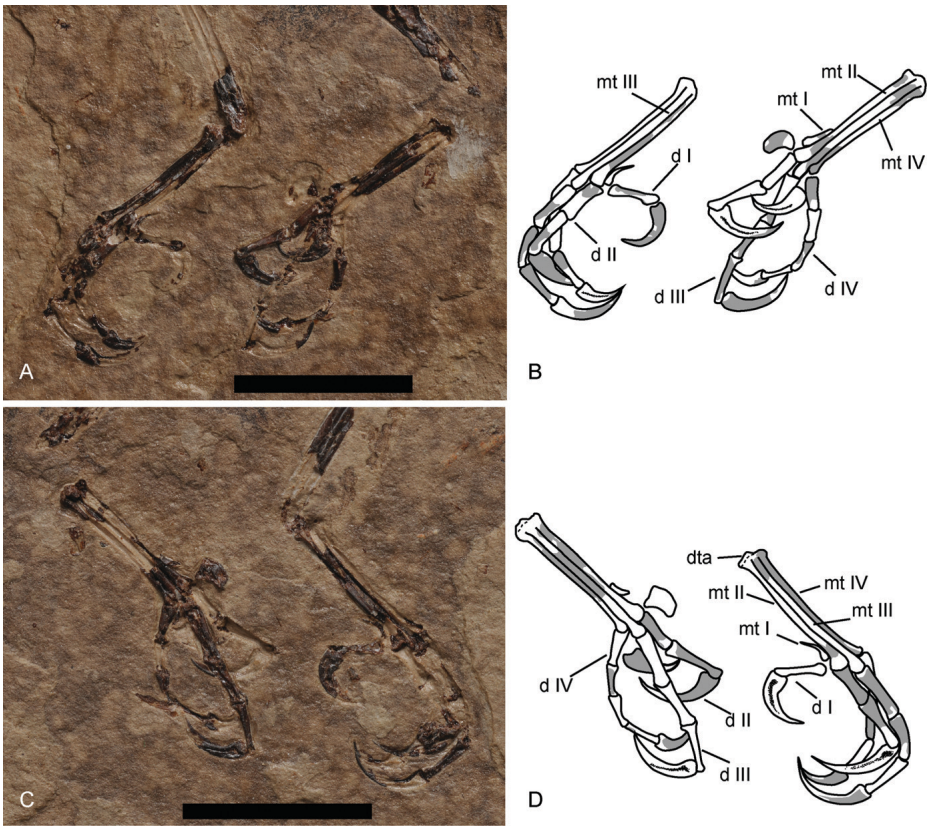

FIGURE 5. Photographs and line drawing of the metatarsals and pedal digits of IVPP V18586, holotype of *Parvavis chuxiongensis*, gen. et sp. nov. **A** and **B**, part; **C** and **D**, counterpart. **Abbreviations**: **d I–IV**, digits I–IV; **mt I–IV**, metatarsals I–IV. All scale bars equal 10 mm.

HISTOLOGICAL DESCRIPTION

The humeral and ulnar midshaft sections taken from this specimen of *Parvavis* all show that the compacta is composed of parallel-fibered bone tissue, and lacks observable vascular canals (Fig. 6). Osteocyte lacunae are arranged in an orderly manner. Flattened and globular lacunae are visible, but the former are overwhelmingly predominant in number. The two types of lacunae are mixed together (Chinsamy et al., 1994, 1995). The two types are separated in *Concornis*, with flattened and globular lacunae in the external and the internal parts of the cortex respectively (Cambra-Moo et al., 2006). Neither lines of arrested growth (LAGs) nor secondary osteons are present. Relative bone wall thickness cannot be measured because the bone shafts are severely compacted.

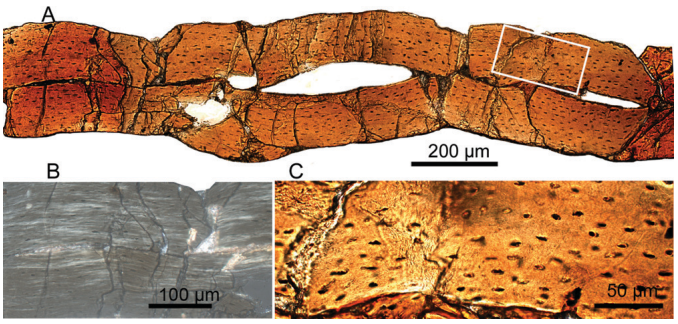

FIGURE 6. Humeral histology of IVPP V18586, holotype of *Parvavis chuxiongensis*, gen. et sp. nov. **A** and **B**, transverse sections under **A**, normal light and **B**, polarized light; **C**, detail structure of framed region in **A** at higher magnification.

DISCUSSION

Comparisons between *Parvavis* and Other Enantiornithines

The phylogenetic analysis resulted in three most parsimonious trees, the strict consensus tree of which places the new species within Enantiornithes (Fig. 7). The overall topology corresponds well with that obtained by O'Connor et al. (2009), but the large polytomies found previously (e.g., Enantiornithes and Ornithuromorpha) are better resolved here. The new cladogram is generally consistent with the result of previous analyses in the placement of most taxa (Clarke et al., 2006; Zhou and Zhang, 2006b; Zhou et al., 2008, 2010), with the main differences involving the positions of *Sapeornis*, Confuciusornithidae, and *Apsaravis*. Confuciusornithidae and *Sapeornis* are recovered as successively more derived basal pygostylians, with *Sapeornis* representing the sister taxon of Ornithothoraces (as in Gao et al., 2008). In contrast, *Sapeornis* was posited to be more basal than the Confuciusornithidae in previous analyses (Clarke et al., 2006; Zhou et al., 2008), and possibly even basal to the long tailed *Jeholornis* (Zhou et al., 2010). *Apsaravis* emerged in a more basal position than *Hongshanornis*, a surprising result in light of recent analyses (Zhou and Zhang, 2005; Clarke et al., 2006; O'Connor et al., 2010; O'Connor and Zhou, 2013).

The Ornithothoraces consists of the clades Enantiornithes and Ornithuromorpha, whose internal relationships are better resolved here than in previous analyses that have used other versions of the same data matrix (O'Connor et al., 2009; You et al., 2010; Ji et al., 2011). Enantiornithes contains two groups, Longipterygidae and an unnamed clade comprising the rest of the enantiornithine birds. Within Longipterygidae (O'Connor et al., 2011), *Shanweiniao* and *Longipteryx* emerge as successive outgroups of the more exclusive clade comprising *Rapaxavis* and *Longirostravis*. However, only two unambiguous

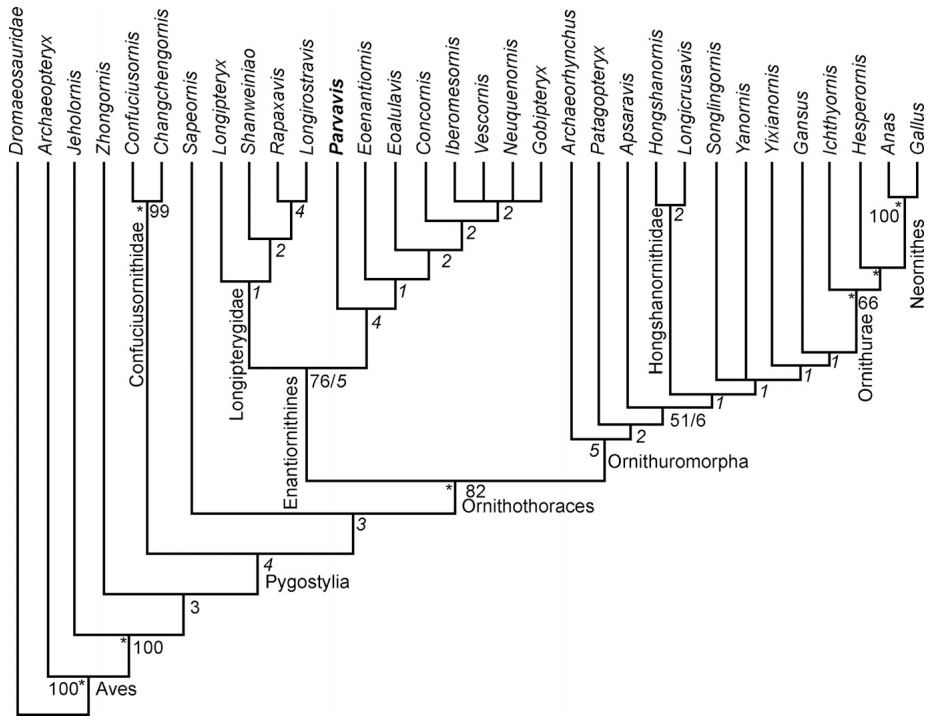

FIGURE 7. Strict consensus of three most parsimonious trees (tree length = 610, consistency index = 0.47, retention index = 0.67), illustrating the phylogenetic position of *Parvavis chuxiongensis*, gen. et sp. nov. Bootstrap values that exceed 50% are shown in normal font under the corresponding nodes. Absolute Bremer support values are indicated in bold italic under the corresponding nodes. We limited our searches for suboptimal trees to trees no more than eight steps longer than the shortest tree (see Materials and Methods). Nodes in the strict consensus tree with Bremer values greater than eight are shown by *.

synapomorphies (character 5:1, upper dentition restricted to the premaxilla; character 79:1, caudally constricted pygostyle) support Longipterygidae, and this clade only has a Bremer value of 1 and a bootstrap value of less than 50%.

The non-longipterygid enantiornithine birds, including *Parvavis*, form the second enantiornithine clade. This grouping formed a large polytomy in the analysis of O'Connor et al. (2009), but is better resolved here. The clade has relatively strong support, requiring additional four steps to collapse it. *Concornis*, *Eoalulavis*, *Eoenantiornis*, and *Parvavis* form successive outgroups to a polytomy of derived taxa (*Iberomesornis*, *Vescornis*, *Neuquenornis*, and *Gobipteryx*). Adding *Parvavis* to the matrix has evidently resulted in improved resolution within Enantiornithes, although this part of the cladogram has low bootstrap support (less than 50% for all nodes within Enantiornithes) and some nodes will collapse in suboptimal trees one or two steps longer.

The topology obtained for Enantiornithes is different from that recovered by O'Connor and Zhou (2013), who used the same data matrix with a few modifications and a larger number of taxa. These authors obtained a more pectinate topology within Enantiornithes, lacking the major dichotomy between longipterygid and non-longipterygid enantiornithines recovered in the present study. The Longipterygidae of O'Connor and Zhou (2013) consisted only of *Longipteryx* and *Boluochia*, with *Shanweiniao*, *Longirostravis*, and *Rapaxavis* falling outside the group. The elongated rostrum, restriction of the upper dentition to the premaxilla, and configuration of the distal trochleae of the metatarsals suggest close affinity among all these taxa (Ji et al., 2011; O'Connor et al., 2011), although these characters may have been independently acquired through adaptation to similar ecological niches. The interrelationships recovered by O'Connor and Zhou (2013) are weakly supported: the clades Enantiornithes and Ornithuromorpha each have a Bremer value of 1, and all the nodes within Enantiornithes have zero Bremer value. Although studies that sample large numbers of taxa are to be welcomed, and have the potential to improve our understanding of the phylogeny of Enantiornithes, including taxa that are too fragmentary or otherwise problematic can result in a highly polytomous strict consensus tree, obscuring true relationships (Wilkinson, 2003). Specifically, the analysis of O'Connor (2009), which included nearly all known enantiornithines, generated a strict consensus tree with a large polytomy. Our analysis of the smaller matrix based on that of O'Connor et al. (2009) was limited to relatively well-known taxa and was more informative with regard to enantiornithine phylogeny.

Ornithuromorpha interrelationships are well resolved by our analysis, and our result is essentially consistent with those of previous analyses, except in the case of *Apsaravis* (Zhou et al., 2009; S. Zhou et al., 2012). The unsolved polytomy obtained by O'Connor et al. (2009) probably resulted from insufficient sampling of Ornithuromorpha, and we attempted to solve this problem by adding *Archaeorhynchus* and *Songlingornis* to the matrix based on information from previous studies (You et al., 2010; Ji et al., 2011). *Archaeorhynchus* is recovered as the basalmost member of Ornithuromorpha (Zhou et al., 2010; Hu et al., 2012; O'Connor and Zhou, 2013). The interrelationships among *Yanornis*, *Yixianornis*, and *Songlingornis* recovered in previous analysis (Clarke et al., 2006) are not fully corroborated by our result. We recovered *Gansus* rather than *Apsaravis* as the sister taxon of Ornithurae, the group in which neornithines are nested, and *Apsaravis* has ended up in a much more basal position.

In our analysis, the clade Enantiornithes is supported by 12 synapomorphies, three of which can be seen in the *Parvavis* holotype: the proximal margin of the humeral head is concave, rising dorsally and ventrally (character 122:1); the width of the deltopectoral crest is narrower than that of the humeral shaft (character 128:0); and the ventrodistal margin of the humerus projects farther distally than the dorsodistal margin, so that the distal surface angles strongly dorsally (character 138:1). Within Enantiornithes, three features optimized as synapomorphies supporting the non-longipterygid clade, and all are present in *Parvavis*: (1) well-developed olecranon fossa (character 135:1); (2) metatarsal IV mediolaterally narrower than metatarsals II and IV (character 226:1); and (3) trochlea of metatarsal II broader than that of metatarsal III (character 236:1). Detailed

TABLE 1. Measurements (mm) of IVPP V18586, holotype of *Parvavis chuxiongensis*, gen. et sp. nov.

Element	Length	Element	Length
Humerus	18.4	Digit II-3	4.5
Radius	18.42	Digit III-1	3.1
Ulna	18.6	Digit III-2	2.6
Femur	14.5	Digit III-3	2.5
Tibiotarsus	17.7	Digit III-4	4.2
Metatarsal III	9.5	Digit IV-1	1.7
Digit I-1	2.6	Digit IV-2	1.7
Digit I-2	3.0	Digit IV-3	1.9
Digit II-1	2.3	Digit IV-4	1.9
Digit II-2	3.1	Digit IV-5	2.9

comparisons with previously known non-longipterygid enantiornithine birds, including species not in the data matrix of O'Connor et al. (2009), are provided in the following paragraphs in order to augment the diagnosis and further distinguish *Parvavis* from other members of this clade.

The deltopectoral crest of the humerus is less well developed in *Parvavis* than in other enantiornithines, including *Otogornis*, *Vescornis*, and *Cathayornis*. The deltopectoral crest is a site of attachment for flight muscles, and its poor development may imply that only weak flight capability was present in *Parvavis*. The fact that the crest does not has an abrupt termination distinguishes *Parvavis* from *Enantiornis leadi*, the El Brete species, *Shenqiornis*, *Protopteryx*, and an unnamed specimen from the Xiagou Formation of China (CAGS-IG-02-0901). *Parvavis* has elongated forelimbs, and the intermembral radio (humeral + ulna/femur + tibiotarsus) of 1.15 (Tables 1, 2) falls within the range known for Longipterygidae (1.07–1.51; O'Connor, 2009), and is considerably larger than the equivalent ratio in *Eoenantiornis*, *Paraprotopteryx*, and *Vescornis* (Table 2).

The three major metatarsals of *Parvavis* can be easily distinguished from the metatarsals of the El Brete enantiornithine birds (Chiappe, 1992, 1993). Known enantiornithine metatarsals from El Brete are generally robust, especially for metatarsal II, and there is a fenestra between the proximal halves of metatarsals III and IV, and the distal ends of metatarsals II and IV deviate from that of metatarsal III. In *Parvavis*, metatarsal II is straight and firmly abuts metatarsal III, and the distal part of the former element lacks the medial curvature seen in *Vescornis*, *Concornis*, and *Gobipteryx*. Metatarsal III is the longest of the metatarsals, its entire trochlea extending distal to the ends of both metatarsals II and IV, a configuration that is completely different from that of longipterygid metatarsal trochleae (O'Connor et al., 2011). *Parvavis* differs from *Qiliania* in possessing proportionally shorter metatarsals (the ratio of metatarsal III/tibiotarsus is 53%, but 63% in *Qiliania*) and in lacking a plantar excavation on the metatarsus (Ji et al., 2011).

Parvavis shares the following features of its pedal phalanges with *Shanweiniao*, *Rapaxavis*, and *Qiliania*: slender digit I; large and slightly curved claws with a longitudinal crest on the medial and lateral surface; and the proximal three phalanges in digit IV equally short (unclear in *Qiliania*, because the first phalanx in digit IV is not exposed). In *Shanweiniao* and *Rapaxavis*, the penultimate phalanx of each digit is longer than the preceding phalanx, but in *Parvavis* and *Qiliania* this is true only of digit III. In *Parvavis* and *Qiliania*, the ungual of digit IV is reduced to the point of being much smaller than the other unguals, a highly unusual features that has otherwise been reported only in *Vescornis* (Ji et al., 2011).

The characters that distinguish *Parvavis* from other enantiornithines do not appear strongly susceptible to ontogenetic variation. In any case, the holotype of *Parvavis* probably represents a subadult rather than a juvenile (see next section), and is therefore unlikely to show large ontogenetic differences from the adult condition. Thus, the erection of a new genus and species for IVPP V18586 is warranted. It is notable that *Parvavis* represents the only known enantiornithine bird form the Upper Cretaceous of China. The fact that our phylogenetic analysis placed *Parvavis* at the base of a non-longipterygid clade otherwise made up primarily of Early Cretaceous taxa implies an interesting mismatch between phylogeny and stratigraphy, and suggests that southern China might have served in the Late Cretaceous as a refugium for enantiornithines that retained many primitive features. However, this issue needs more study, especially rigorous phylogenetic analysis of a larger sample of enantiornithines, ideally including new specimens from the Upper Cretaceous of southern China.

TABLE 2. Proportions of selected elements of *Parvavis chuxiongensis*, gen. et sp. nov., in comparison with other enantiornithine birds (lengths are measured in millimeters).

Taxon	Hu	Ul	Fe	Ti	Hu + Ul/ Fe + Ti
Parvavis (IVPP V18586)	18/R	19/R	14/R	18/R	1.15
Shanweiniao (DMNH D1878)	22/R	23*/R	18*/L	23/L	1.10
Paraprotopteryx (STM V001)	23	23	22	26	0.96
Rapaxavis (DMNH D2522)	23/L	23/L	19/L	23/L	1.09
Cathayornis (IVPP V9769)	27/R	28/R	24	29	1.04
Eoenantiornis (IVPP V11537)	30/L	31/L	27/L	33/L	1.02
Longipteryx (IVPP V12325)	45/R	47/R	31/R	32/R	1.3
Pengornis (IVPP V15536)	65/R	70/R	45/R	50/R	1.42
Vescornis (NIGP CAS130722)	24	24	23	27	0.96
Sinornis (BNHM BPV538)	24/R	19*/L	21/R	26/R	0.91
Iberomesornis (LH 22)			15	20	
Concornis (LH 2814)		32*	25*	31*	

Abbreviations: **Fe**, femur; **Hu**, humerus; **L** and **R**, left and right; **Ti**, tibiotarsus; **Ul**, ulna. The data for *Iberomesornis*, *Concornis*, *Sinornis*, *Longipteryx*, *Vescornis*, *Paraprotopteryx*, *Rapaxavis*, and *Shanweiniao* are measured from figures in the literature (Sanz and Buscalioni, 1992; F. Zhang et al., 2001, 2004; Sereno et al., 2002; Zheng et al., 2007; Morschhauser et al., 2009; O'Connor et al., 2009). * = estimated.

Ontogenetic Status of the *Parvavis* Holotype

Only four enantiornithine birds have been previously subjected to histological analysis. A prenatal *Gobipteryx* was found to resemble modern birds in possessing well-vascularized woven bone tissue (Chinsamy and Elzanowski, 2001). Two adults studied by Chinsamy et al. (1994, 1995) exhibited poorly vascularized parallel-fibered bone with LAGs. An adult *Concornis* specimen exhibited an outer layer of parallel-fibered tissue with LAGs, as seen in Chinsamy et al. (1994, 1995), and an inner layer vascularized by secondary osteons (Cambra-Moo et al., 2006). The histological information provided by these samples pertains to extreme ontogenetic stages, prenatal or adult, and the intermediate stages are hardly known. In *Parvavis*, the cortex of the humerus and ulna consist entirely of parallel-fibered bone without LAGs, as in the internal cortices of the adult enantiornithine bones studied by Chinsamy et al. (1994, 1995), but in contrast to the internal cortex of *Concornis* (Cambra-Moo et al., 2006). In the four adult enantiornithines studied by Chinsamy et al. (1994, 1995) and Cambra-Moo et al. (2006), the internal cortex is circumscribed by the outer lamellar bone with LAGs. The holotype of *Parvavis* has evidently passed the fast-growing stage, and the remodeling process has completely resorbed the initial woven or fibrolamellar bone tissue formed during the early stage. The absence of LAGs indicates that growth had not yet paused, although it had slowed down substantially, in the *Parvavis* holotype. This unusual condition could be interpreted in a number of ways. One possibility is that the specimen is actually mature. This might imply that the growth stoppages (LAGs) seen in the other adult

enantiornithine specimens that have been studied histologically were caused by outside influences, such as food shortages or periods of unfavorable climatic conditions, as occurs in modern kiwi and wild ruminants (Bourdon et al., 2009; Köhler et al., 2012). Alternatively, the *Parvavis* holotype may not have reached the ontogenetic stage at which growth stoppages first occurred in enantiornithines, implying that other specimens represent the normal adult condition (Chinsamy-Turan, 2005). Considering that free distal tarsals like those present in the *Parvavis* holotype are rarely seen in adult enantiornithines, and LAGs are present in all adult enantiornithines that have been previously studied histologically, the second explanation appears more reasonable. Thus, the *Parvavis* holotype actually supplements our understanding of enantiornithine histology by providing information about the subadult condition. The *Parvavis* holotype differs from a recently reported subadult specimen of *Sapeornis* (DNHM-D3078; Gao et al., 2012), in lacking an inner layer of woven-textured tissue and in having less vascularized bone tissue. These differences suggest that the *Parvavis* holotype may have been closer to adulthood than the subadult *Sapeornis* at the time of death. Such cross-taxon comparisons are not strictly justified, however.

Enantiornithes is a diverse group in need of both morphological and ontogenetic investigation. Even counting the present study, histological research has been performed on only a few enantiornithine specimens (Chinsamy et al., 1994, 1995; Chinsamy and Elzanowski, 2001; Cambra-Moo et al., 2006), which derive from a variety of taxa and mainly represent extreme ontogenetic stages (embryo or adult). The available histological information is far from sufficient to allow a complete growth series to be reconstructed for any enantiornithine, a step that will be important for understanding enantiornithine physiology and other biological issues. The ontogenetic status of a given specimen cannot be fully determined purely on the basis of histological features. For that, evidence from bone surface texture and fusion of compound bones should also be taken into account (Tumarkin-Deratzian et al., 2006). The *Parvavis* holotype is extremely small, being comparable in size to the juvenile enantiornithine specimens GMV-2158 and GMV-2156 (Chiappe et al., 2007b), but lacks evident foramina or striations on the periosteal bone surfaces, even on the articular areas. These features characteristically occur in juvenile or younger individuals (Tumarkin-Deratzian et al., 2006; Chiappe et al., 2007b), so their absence in the *Parvavis* holotype is an indication of relative maturity. The fusion of the distal tarsals and metatarsals seen in adult enantiornithines contrasts with the existence of free distal tarsals in juvenile specimens and suggests that fusion in this part of the skeleton is subject to ontogenetic variation (Chiappe and Walker, 2002; Chiappe et al., 2007b). The minimal amount of tarsometatarsal fusion in the *Parvavis* holotype suggests subadult rather than adult status. More studies of subadult enantiornithines will be needed in order to determine whether it represents the early or later part of the subadult stage. However, it is evident that tarsometatarsal fusion happens relatively late in ontogeny. In modern birds, which grow fast enough that they usually reach adult size within a year, LAGs do not normally occur (Chinsamy et al., 1995). This makes it difficult to interpret the physiological causes and implications of the LAGs that have been seen in adult enantiornithine birds. Numerous studies have confirmed that annual LAGs are characteristic of squamates, crocodilians, and non-avian dinosaurs (Castanet, 1994; Erickson et al., 2004; Erickson, 2005), and the rule of annual formation should also be applicable to LAGs seen in primitive birds. If this is true, it would imply that the holotype individual of *Parvavis* was less than a year old at the time of death.

Histological studies suggest that enantiornithines grew fast during early development (prenatal *Gobipteryx*; Chinsamy and Elzanowski, 2001), but that later growth was slower and involved periodical stoppages (indicated by parallel-fibered bone and LAGs; Chinsamy-Turan, 2005). Some individuals may have reached a significant percentage of full body size by the end of the initial fast-growing stage (Cambra-Moo et al., 2006), as indicated by the small difference in body size between juvenile (IVPP V12552) and adult (IVPP V12325) individuals of *Longipteryx* (10% size difference; O'Connor et al., 2011). To date, *Longipteryx* is the only enantiornithine in which specimens at different ontogenetic stages have been compared, although this case study would be even more valuable if the specimens had been investigated histologically.

As a subadult, the holotype individual of *Parvavis* should be even closer to adult size than the juvenile *Longipteryx* studied by O'Connor et al. (2011). Even assuming a 10% size difference between the holotype and a conspecific adult, the tibiotarsus of an adult *Parvavis* would still be shorter than that of the holotype of *Iberomesornis* (Sanz and Buscalioni, 1992). Given that *Iberomesornis* was previously the smallest known enantiornithine, and that the holotype of this taxon probably also represents a subadult (O'Connor, 2009), the adult body size of *Parvavis* may have been smaller than that of any other known enantiornithine bird. Enantiornithes exhibit a general increase in size from Early to Late Cretaceous, which has been linked to the emergence of improved flight ability over the course of their evolution (Chiappe and Walker, 2002). The minute size of *Parvavis* becomes particularly intriguing and distinctive when this taxon is compared with its turkey-sized enantiornithine contemporaries. Considering that only limited information is currently available regarding enantiornithine growth series, the extremely small holotype of *Parvavis* still contributes to our understanding of the diversity in body size that existed among enantiornithine birds.

ACKNOWLEDGMENTS

We are truly grateful to Y. Li and Y.-T. Li for fossil preparation, J. Zhang for photos, X.-Z. Liu for making a partial cast of the *Parvavis* holotype, S.-K. Zhang for preparing histological sections, and J. K. O'Connor and F.-L. Han for discussion. We thank C. Sullivan for reading and editing the manuscript. This research was supported by the National Basic Research Program of China (973 Program, 2012CB821906), and the National Natural Science Foundation of China. We thank the editor T. Worthy and reviewers C. Sullivan and E. Morschhauser for reviewing the manuscript and providing helpful comments.

LITERATURE CITED

Baumel, J. J., and L. M. Witmer. 1993. Osteologia; pp. 45–132 in J. J. Baumel, A. S. King, J. E. Breazile, H. E. Evans, and J. C. Vanden Berge (eds.), Handbook of Avian Anatomy: Nomina Anatomica Avium, second edition. Nuttall Ornithological Club, Cambridge, U.K.

Bourdon, E., J. Castanet, A. de Ricqlès, P. Scofield, A. Tennyson, H. Lamrous, and J. Cubo. 2009. Bone growth marks reveal protracted growth in New Zealand kiwi (Aves, Apterygidae). Biology Letters 5:639–642.

Bremer, K. 1994. Branch support and tree stability. Cladistics 10:295–304.

Cambra-Moo, O., Á. D. Buscalioni, J. Cubo, J. Castanet, M.-M. Loth, E. de Margerie, and A. de Ricqlès. 2006. Histological observations of enantiornithine bone (Saurischia, Aves) from the Lower Cretaceous of Las Hoyas (Spain). Comptes Rendus Palevol 5:685–691.

Castanet, J. 1994. Age estimation and longevity in reptiles. Gerontology 40:174–192.

Chen, P. 2000. Comments on the classification and correlation of nonmarine Jurassic and Cretaceous of China. Journal of Stratigraphy 24:114–119. [Chinese]

Chiappe, L. M. 1992. Enantiornithine (Aves) tarsometatarsi and the avian affinities of the Late Cretaceous Avisauridae. Journal of Vertebrate Paleontology 12:344–350.

Chiappe, L. M. 1993. Enantiornithine (Aves) tarsometatarsi from the Cretaceous Lecho Formation of northwest Argentina. American Museum Novitates 3083:1–27.

Chiappe, L. M., and J. O. Calvo. 1994. *Neuquenornis volans*, a new Late Cretaceous bird (Enantiornithes: Avisauridae) from Patagonia, Argentina. Journal of Vertebrate Paleontology 14:230–246.

Chiappe, L. M., and C. A. Walker. 2002. Skeletal morphology and systematics of the Cretaceous Euenantiornithes (Ornithothoraces: Enantiornithes); pp. 240–267 in L. M. Chiappe and L. M. Witmer (eds.), Mesozoic Birds: Above the Heads of Dinosaurs. University of California Press, Berkeley, California.

Chiappe, L. M., S. Ji, and Q. Ji. 2007b. Juvenile birds from the Early Cretaceous of China: implications for enantiornithine ontogeny. American Museum Novitates 3594:1–46.

Chiappe, L. M., S. Suzuki, G. J. Dyke, M. Watabe, K. Tsogtbaatar, and R. Barsbold. 2007a. A new enantiornithine bird from the Late Cretaceous of the Gobi desert. Journal of Systematic Palaeontology 5:193–208.

Chinsamy, A., and A. Elzanowski. 2001. Bone histology: evolution of growth pattern in birds. Nature 412:402–403.

Chinsamy, A., L. M. Chiappe, and P. Dodson. 1994. Growth rings in Mesozoic birds. Nature 368:196–197.

Chinsamy, A., L. M. Chiappe, and P. Dodson. 1995. Mesozoic avian bone microstructure: physiological implications. Paleobiology 21:561–574.

Chinsamy-Turan, A. 2005. The Microstructure of Dinosaur Bone. Johns Hopkins University Press, Baltimore, Maryland, 195 pp.

Clarke, J. A., Z. Zhou, and F. Zhang. 2006. Insight into the evolution of avian flight from a new clade of Early Cretaceous ornithurines from China and the morphology of *Yixianornis grabaui*. Journal of Anatomy 208:287–308.

Erickson G. M. 2005. Assessing dinosaur growth patterns: a microscopic revolution. Trends in Ecology and Evolution 20:677–684.

Erickson G. M., P. J. Makovicky, P. J. Currie, M. A. Norell, S. A. Yerby, and A. B. Christopher. 2004. Gigantism and comparative life-history parameters of tyrannosaurid dinosaurs. Nature 430:772–775.

Forster, C. A., S. D. Sampson, L. M. Chiappe, and D. W. Krause. 1998. The theropodan ancestry of birds: new evidence from the Late Cretaceous of Madagascar. Science 279:1915–1919.

Gao, C., L. M. Chiappe, Q. Meng, J. K. O'Connor, X. Wang, X. Cheng, and J. Liu. 2008. A new basal lineage of Early Cretaceous birds from China and its implications on the evolution of the avian tail. Palaeontology 51:775–791.

Gao, C., L. M. Chiappe, F. Zhang, D. L. Pomeroy, C. Shen, A. Chinsamy, and M. O. Walsh. 2012. A subadult specimen of the Early Cretaceous bird *Sapeornis chaoyangensis* and a taxonomic reassessment of sapeornithids. Journal of Vertebrate Paleontology 32: 1103–1112.

Giannini, N. P., S. Bertilli, and S. J. Hackett. 2004. Phylogeny of extant penguins based on integumentary and breeding characters. Auk 121:422–434.

Goloboff, P. A., J. S. Farris, and K. C. Nixon. 2008. TNT, a free program for phylogenetic analysis. Cladistics 24:774–786.

Harris J. D., M. C. Lamanna, H. You, S. Ji, and Q. Ji. 2006. A second enantiornithean (Aves: Ornithothoraces) wing from the Early Cretaceous Xiagou Formation near Changma, Gansu Province, People's Republic of China. Canadian Journal of Earth Sciences 43:547–554.

Hou, L. 1994. A Late Mesozoic bird from Inner Mongolia. Vertebrata PalAsiatica 32:258–266.

Howard, H. 1929. The avifauna of Emeryville shell mound. University of California. Publications in Zoology 32:301–394.

Hu, D., X. Xu, L. Hou, and C. Sullivan. 2012. A new enantiornithine bird from the Lower Cretaceous of western Liaoning, China, and its implications for early avian evolution. Journal of Vertebrate Paleontology 32:639–645.

Ji, S. A., J. Atterholt, J. K. O'Connor, M. C. Lamanna, J. D. Harris, D. Q. Li, H. You, and P. Dodson. 2011. A new, three-dimensionally preserved enantiornithine bird (Aves: Ornithothoraces) from Gansu Province, north-western China. Zoological Journal of the Linnean Society 162:201–219.

Köhler, M., N. Marin-Moratalla, X. Jordana, and R. Aanes. 2012. Seasonal bone growth and physiology in endotherms shed light on dinosaur physiology. Nature 487:358–361.

Lamanna, M. C., H. You, J. D. Harris, L. M. Chiappe, S. Ji, L. Chang, and Q. Ji. 2006. A partial skeleton of an enantiornithine bird from the Early Cretaceous of northwestern China. Acta Palaeontologica Polonica 51:423–433.

Li, J., Z. Li, Y. Zhang, Z. Zhou, Z. Bai, L. Zhang, and T. Ba. 2008. A new species of *Cathayornis* from Lower Cretaceous of Inner Mongolia, China and its stratigraphic significance. Acta Geologica Sinica 82:1115–1123.

Linnaeus, C. 1758. Systema Naturae per Regna Tria Naturae, Secundum Classes, Ordines, Genera, Species, cum Characteribus, Differentiis, Synonymis, Locis. Volume 1: Regnum Animale. Editio decima, reformata. Laurentii Salvii, Stockholm, 824 pp.

Morschhauser, E. M., D. J. Varricchio, C. Gao, J. Liu, X. Wang, X. Cheng, and Q. Meng. 2009. Anatomy of the Early Cretaceous bird *Rapaxavis pani*, a new species from Liaoning province, China. Journal of Vertebrate Paleontology 29:545–554.

O'Connor, J. K. 2009. A systematic review of Enantiornithes (Aves: Ornithothoraces). Ph.D. dissertation, University of Southern California, Los Angeles, California, 600 pp.

O'Connor, J. K., and L. M. Chiappe. 2011. A revision of enantiornithine (Aves: Ornithothoraces) skull morphology. Journal of Systematic Palaeontology 9:135–157.

O'Connor, J. K., and Z. Zhou. 2013. A redescription of *Chaoyangia beishanensis* (Aves) and a comprehensive phylogeny of Mesozoic birds. Journal of Systematic Palaeontology 11:889–906.

O'Connor, J. K., K. Gao, and L. M. Chiappe. 2010. A new ornithuromorph (Aves: Ornithothoraces) bird from the Jehol Group indicative of higher-level diversity. Journal of Vertebrate Paleontology 30:311–321.

O'Connor, J. K., L. M. Chiappe, C. Gao, and B. Zhao. 2011. Anatomy of the Early Cretaceous enantiornithine bird *Rapaxavis pani*. Acta Palaentologica Polonica 56:463–475.

O'Connor, J. K., X. Wang, L. M. Chiappe, C. Gao, Q. Meng, X. Cheng, and J. Liu. 2009. Phylogenetic support for a specialized clade of Cretaceous enantiornithine birds with information from a new species. Journal of Vertebrate Paleontology 29:188–204.

Sanz, J. L., and J. F. Bonaparte. 1992. A new order of birds (Class: Aves) from the Lower Cretaceous of Spain. Natural History Museum of Los Angeles County Science Series 36:39–49.

Sanz, J. L., and A. D. Buscalioni. 1992. A new bird from the Early Cretaceous of Las Hoyas, Spain. Paleontology 35:829–845.

Sanz, J. L., B. P. Perez-Moreno, L. M. Chiappe, and A. Buscalioni. 2002. The birds from the Lower Cretaceous of Las Hoyas (Province of Cuenca, Spain); pp. 209–229 in L. M. Chiappe and L. M. Witmer (eds.), Mesozoic Birds: Above the Heads of Dinosaurs. University of California Press, Berkeley, California.

Sereno, P. C. 2000. *Iberomesornis romerali* (Aves, Ornithothoraces) reevaluated as an Early Cretaceous enantiornithine. Neues Jarhbuch für Geologie und Paläontologie Abhandlungen 215:365–395.

Sereno, P. C., C. Rao, and J. Li. 2002. *Sinornis santensis* (Aves: Enantiornithes) from the Early Cretaceous of Northeastern China; pp. 184–208 in L. M. Chiappe and L. M. Witmer (eds.), Mesozoic Birds: Above the Heads of Dinosaurs. University of California Press, Berkeley, California.

Tumarkin-Deratzian, A. R., D. R. Vann, and P. Dodson. 2006. Bone surface texture as an ontogenetic indicator in long bones of the Canada goose *Branta canadensis* (Anseriformes: Anatidae). Zoological Journal of the Linnean Society 148:133–168.

Walker, C. A. 1981. New subclass of birds from the Cretaceous of South America. Nature 292:51–53.

Walker, C. A., E. Buffetaut, and G. J. Dyke. 2007. Large euenantiornithine birds from the Cretaceous of southern France, North America and Argentina. Geological Magazine 144:977–986.

Wang, X., J. K. O'Connor, B. Zhao, L. M. Chiappe, C. Gao, and X. Cheng. 2010. New species of enantiornithes (Aves: Ornithothoraces) from the Qiaotou Formation in northern Hebei, China. Acta Geologica Sinica 84:247–256.

Wellnhofer, P. 1992. A new specimen of *Archaeopteryx* from the Solnhofen Limestone; pp. 3–23 in K. E. Campbell (ed.), Papers in Avian Paleontology Honoring Pierce Brodkorb. Science Series Natural History, Museum of Los Angeles County 36.

Wilkinson, M. 2003. Missing entries and multiple trees: instability, relationships, and support in parsimony analysis. Journal of Vertebrate Paleontology 23:311–323

You, H., J. K. O'Connor, L. M. Chiappe, and Q. Ji. 2005. A new fossil bird from the Early Cretaceous of Gansu province, northwestern China. Historical Biology 17:7–14.

You, H., J. Atterholt, J. K. O'Connor, J. D. Harris, M. C. Lamanna, and D. Q. Li. 2010. A second Cretaceous ornithuromorph bird from the Changma Basin, Gansu Province, northwestern China. Acta Palaeontologica Polonica 55:617–625.
Zhang, F., and Z. Zhou. 2000. A primitive enantiornithine bird and the origin of feathers. Science 290:1955–1959.
Zhang, F., P. G. Ericson, and Z. Zhou. 2004. Description of a new enantiornithine bird from the Early Cretaceous of Hebei, northern China. Canadian Journal of Earth Sciences 41:1097–1107.
Zhang, F., Z. Zhou, L. Hou, and G. Gu. 2001. Early diversification of birds: evidence from a new opposite bird. Chinese Science Bulletin 46:945–949.
Zhang, M., P. Chen, Y. Wang, and Y. Wang (eds.). 2001. The Jehol Biota. Shanghai Science and Technology Publishers, Shanghai, China, 208 pp.
Zhang, Y.-Z. (ed.). 1996. Stratigraphy of Yunnan Province. China University of Geosciences Press, Wuhan, China, 366 pp.
Zheng, X., Z. Zhang, and L. Hou. 2007. A new enantiornitine bird with four long rectrices from the Early Cretaceous of northern Hebei, China. Acta Geologica Sinica 81:703–708.
Zhou, S., Z. Zhou, and J. K. O'Connor. 2012. A new basal beaked ornithurine bird from the Lower Cretaceous of western Liaoning, China. Vertebrata PalAsiatica 50:9–24.
Zhou, Z. 1995. The discovery of Early Cretaceous birds in China. Courier Forschungsinstitut Senckenberg 181:9–22.
Zhou, Z. 2002. A new and primitive enantiornithine bird from the Early Cretaceous of China. Vertebrata PalAsiatica 22:49–57.
Zhou, Z. 2006. Evolutionary radiation of the Jehol Biota: chronological and ecological perspectives. Geological Journal 41:377–393.
Zhou, Z., and F. Zhang. 2005. Discovery of an ornithurine bird and its implication for Early Cretaceous avian radiation. Proceedings of the National Academy of Sciences of the United States of America 102:18998–19002.
Zhou, Z., and F. Zhang. 2006a. Mesozoic birds of China—a synoptic review. Vertebrata PalAsiatica 44:74–98.
Zhou, Z., and F. Zhang. 2006b. A beaked basal ornithurine bird (Aves, Ornithurae) from the Lower Cretaceous of China. Zoologica Scripta 35:363–373.
Zhou, Z., P. M. Barrett, and J. Hilton. 2003. An exceptionally preserved Lower Cretaceous ecosystem. Nature 421:807–814.
Zhou, Z., L. M. Chiappe, and F. Zhang. 2005. Anatomy of the Early Cretaceous bird *Eoenantiornis buhleri* (Aves: Enantiornithes) from China. Canadian Journal of Earth Sciences 42:1331–1338.
Zhou, Z., J. Clarke, and F. Zhang. 2008. Insight into diversity, body size and morphological evolution from the largest Early Cretaceous enantiornithine bird. Journal of Anatomy 212:565–577.
Zhou, Z., F. Jin, and J. Zhang. 1992. Preliminary report on a Mesozoic bird from Liaoning, China. Chinese Science Bulletin 37: 1365–1368.
Zhou, Z., F. Zhang, and Z. Li. 2009. A new basal ornithurine bird (*Jianchangornis microdonta* gen. et sp. nov.) from the Lower Cretaceous of China. Vertebrata PalAsiatica 47:299–310.
Zhou, Z., F. Zhang, and Z. Li. 2010. A new Lower Cretaceous bird from China and tooth reduction in early avian evolution. Proceedings of the Royal Society B: Biological Sciences 277:219–227.

Submitted November 8, 2012; revisions received April 1, 2013; accepted April 6, 2013.
Handling editor: Trevor Worthy.

APPENDIX 1. Twenty-nine characters scored for *Parvavis chuxiongensis*, gen. et sp. nov., in the data matrix of O'Connor et al. (2009).

70:2, 74:0, 121:0, 122:1, 127:0, 128:0, 129:0, 130:1, 135:1, 136:1, 138:1, 143:1, 144:1, 176:3, 221:0, 223:1, 224:0, 225:0, 226:1, 227:0, 228:0, 229:0, 230:0, 234:0, 235:0, 236:1, 238:0, 239:1, 240:1.